Karadeniz Fen Bilimleri Dergisi, 15(1), 362-381, 2025. DOI: 10.31466/kfbd.1551562

KFBD

Karadeniz Fen Bilimleri Dergisi
The Black Sea Journal of Sciences
ISSN (Online): 2564-7377 https://dergipark.org.tr/tr/pub/kfbd

Araştırma Makalesi / Research Article

Design and Experimental Validation of an Effective Controller for Autonomous Differential Wheeled Robots

Osman ÜNAL[1*]

Abstract

This research focuses on the control of differential wheeled robots and aims to develop a new, practical controller inspired by the well-known PID controller. The primary challenge with traditional PID controllers lies in the difficulty of accurately optimizing the three key parameters (coefficients of Proportional, Integral and Derivative) through experimental trial and error. While numerical simulations offer solutions for parameter optimization, real-world factors such as friction losses, inconsistent current and voltage supply to the DC motors, and wheel slippage often prevent these optimized parameters from achieving the same effectiveness in physical systems. This study proposes a novel controller designed to address these challenges, simplifying the parameter tuning process to a single, easily adjustable variable. The new controller, while inspired by the PID approach, offers an effective alternative, overcoming the limitations posed by real-world conditions. It was implemented and tested on a differential wheeled robot specifically designed for this research. Experimental testing across various tasks demonstrated that the new controller provides stable and reliable control, making it a valuable alternative to traditional PID-based approaches.

Keywords: Differential wheeled robots, PID controller, Simplified Controller Design.

Diferansiyel Tekerlekli Otonom Robotlar için Etkili bir Denetleyicinin Tasarımı ve Deneysel Doğrulaması

Öz

Bu araştırma, diferansiyel tekerlekli robotların denetimine odaklanmakta ve yaygın olarak bilinen PID denetleyiciden esinlenerek yeni ve pratik bir denetleyici geliştirmeyi amaçlamaktadır. Geleneksel PID denetleyicideki temel zorluk, deneysel deneme yanılma yoluyla üç temel parametrenin (Orantı, İntegral ve Türev işlevlerine ait katsayılar) doğru bir şekilde optimize edilmesinin güçlüğünde yatmaktadır. Sayısal benzetimler parametre optimizasyonu için çözümler sunarken, sürtünme kayıpları, DC motorlara tutarsız akım ve voltaj beslemesi ve tekerlek kayması gibi fiziksel gerçek faktörleri, bu optimize edilmiş parametrelerin gerçek hayatta aynı etkinliğe ulaşmasını sıklıkla engellemektedir. Bu çalışma, parametre optimizasyon sürecini tek ve kolayca ayarlanabilir bir değişkene basitleştirerek bu zorlukları ele almak üzere tasarlanmış yeni bir denetleyici önermektedir. PID yaklaşımından esinlenen yeni denetleyici, gerçek dünya koşullarının getirdiği sınırlamaların üstesinden gelerek etkili bir alternatif sunmaktadır. Önerilen denetleyici, bu araştırma için özel olarak tasarlanmış diferansiyel tekerlekli bir robot üzerinde uygulanmış ve test edilmiştir. Çeşitli görevlerde yapılan deneysel testler, yeni denetleyicinin istikrarlı ve etkili denetim sağladığını ve onu geleneksel PID tabanlı yaklaşımlara göre değerli bir alternatif haline getirdiğini göstermiştir.

Anahtar Kelimeler: Diferansiyel tekerlekli robotlar, PID denetleyici, Sadeleştirilmiş Denetleyici Tasarımı.

[1]Sakarya University of Applied Sciences, Maritime Vocational School, Sakarya, Turkiye, osmanunal@subu.edu.tr

[*]Sorumlu Yazar/Corresponding Author

Geliş/Received: 09.10.2024 **Kabul/Accepted:** 12.03.2025 **Yayın/Published:** 15.03.2025

Ünal, O. (2025). Design and Experimental Validation of an Effective Controller for Autonomous Differential Wheeled Robots. *Karadeniz Fen Bilimleri Dergisi*, 15(1), 362-381.

1. Introduction

Differential wheeled robot control has attracted an increasing amount of interest nowadays owing to its widespread application in a variety of fields, such as service robotics, industrial automation, and autonomous navigation (Díaz et al., 2021; Mújica et al., 2021; Zhu et al., 2021). With two independently driven wheels, the differential wheeled robot presents unique challenges for control system design, particularly in terms of precise movement and stability. Traditional control approaches, such as the proportional-integral-derivative (PID) controller, have been frequently employed for this reason. However, optimizing the PID parameters—specifically, the proportional, integral, and derivative gains—remains a difficult issue that frequently relies on experimental trials and error-prone techniques (Joseph et al., 2022; Somefun et al., 2021). This complexity arises from the inherent physical realities encountered in real-world scenarios, such as friction losses, variations in motor performance, and the non-ideal behavior of the robot's wheels during operation, which can lead to discrepancies between simulated and actual performance (Gharghory & Kamal, 2012; Ye et al., 2017; Zhang et al., 2022).

The purpose of this study is to suggest a new control scheme for differential wheeled robots inspired by the PID control scheme which would make the tuning procedure easier due to the fewer parameters needing optimization. Rather than having to tune three parameters, as with the conventional PID controller, the suggested controller only needs one adjustable parameter, which is more flexible for control design. This is expected to improve the robustness of the robot under different working conditions. The efficacy of the proposed controller will be tested on a specially designed differential wheeled robot for this research. The goal of the research is to move towards an application of the simplified control model for differential wheeled robots so as to improve the reliability and efficiency of robotic systems (Ortenzi et al., 2018; Raj & Seamans, 2019; Jin, 2023).

Alongside the controller's design and implementation, this work will also include test drives of the robot completing various tasks in order to assess its performance. These tasks will be chosen to determine the robot's ability to navigate and manipulate in various conditions, thus evaluating the controller's performance comprehensively. It is anticipated that the experimental results will prove that the proposed controller not only provides smooth control but also enables effective adaptation to the sudden changes in terrain that a differential wheeled robot is likely to encounter. This research provides to the robotic control systems by tackling the problem of traditional PID controllers by establishing a more useful real-life application of the phenomena (Zhang, 2015; Sahu & Prusty, 2018; Salman et al., 2019; Carlucho et al., 2021; Ali et al., 2021; Tahtawi et al., 2023).

This research is significant because it suggests a new control approach that has possible repercussions in the field of robotics. With the growing prevalence of robots in our daily lives and

industries, it is no doubt that a good control system will be sought after. This study attempts to improve the design process of control systems for differential wheeled robots so they can be controlled more easily and easily adjusted to in the future. Beyond that, data learned from the experimental testing will be useful for subsequent projects and eventually new ways of controlling robots and their tasks may be developed (Lee and Chen 2015; Mohanty and Parhi 2013; Kesavan et al. 2016; Qu et al. 2023).

Briefly, this study tries to address the issues of managing differential wheeled robots by designing a new controller based on the PID ideology. This implies that the research purposefully tries to validate the approach through experimentation and various tests to prove the stability and effectiveness of the control strategy that will benefit technology in robotics and control engineering.

2. Materials and Methods

A differential wheeled robot is known as a mobile robot that uses two wheels that are independently slaved to either side of its body. Since there are no additional steering mechanisms, these robots can change directions simply by changing the combination of relative rotational speed of the wheels. Robots of this type usually have one or more caster wheels to support the device and prevent it from tipping over (Klancar et al., 2017; Mohanty and Parhi 2013). If both wheels forward and turn at the same angle, the robot will move obediently in a straight line. If the wheels are set to rotate in opposites at equal speeds, the robot will pivot around in a circle towards the middle point of the wheels. Based upon the direction as well as the speed of rotation, the robot’s center of rotation can lie along the line connecting the two contact points of the wheels. If the robot is in linear movement, then the point of rotation has an infinitely distant location from the robot. Because the direction of the robot relies on the direction of wheels' rotation as well as the speed, then the variables need to be properly measured and controlled. A differentially steered robot is similar to differential gears of cars in the sense that wheels have the capacity to have speeds in unlike amounts. However, unlike in a differential gear system, both of the wheels in a differentially steered system are powered. These robots are typically found in robotics because their movement is simple to program and control. Nowadays, almost all mobile robots use differential steering owing to its cost-effectiveness and simplicity (Li et al., 2025; Lee et al., 2025; Byeon et al., 2025).

2.1. Kinematics of Differential Drive Robots

Figure 1 illustrates the differential drive kinematics of a mobile wheeled robot. The variables are represented as follows: X and Y denote the global coordinate system, while the robot's orientation

relative to this coordinate system is given by the angle φ. The radius of the wheels is represented by r, and the width of the vehicle by b. Assuming there is no slipping and that the wheels remain in contact with the ground, they trace arcs on the plane, causing the vehicle to rotate around a point known as the Instantaneous Center of Rotation (ICR). The ground contact velocities of the left and right wheels, denoted as V_L and V_R respectively, result in the vehicle rotating with an angular velocity ω.

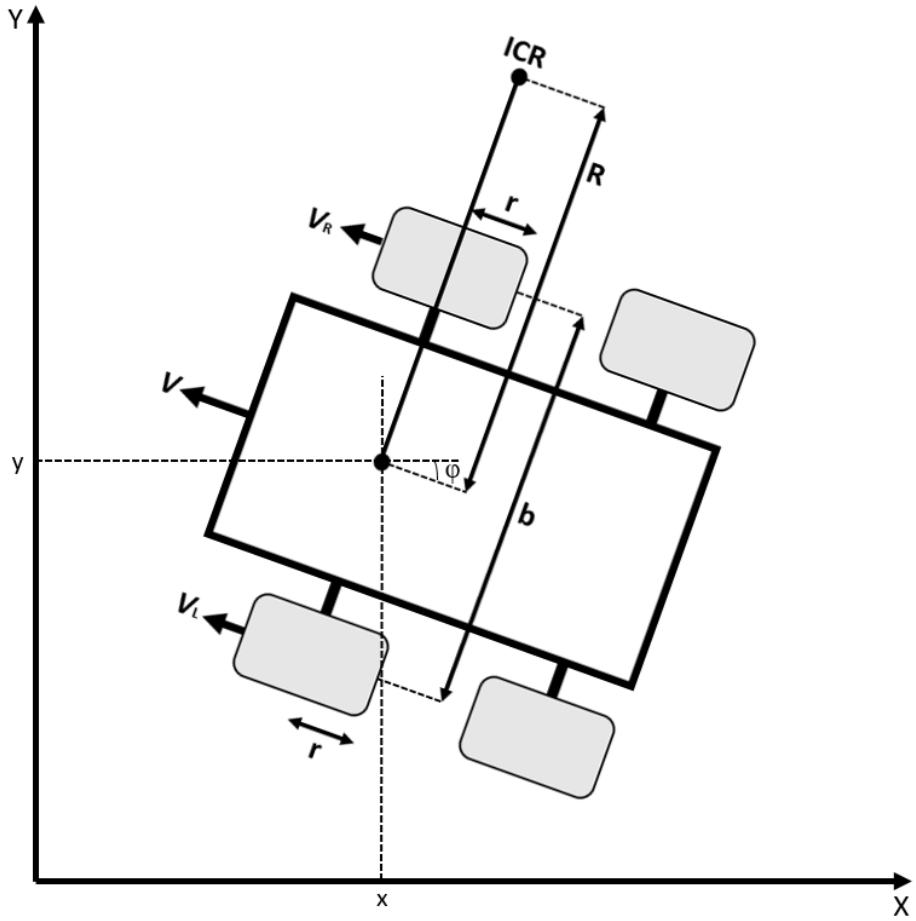

Figure 1. Differential Drive Kinematics.

Based on the definition of angular velocity, the following Equation 1 and Equation 2 can be derived:

$$\omega\left(R+\frac{b}{2}\right)=V_R \tag{1}$$

$$\omega\left(R-\frac{b}{2}\right)=V_L \tag{2}$$

Using the above two equations, obtaining the unknowns ω and R (defined as the distance from the ICR to the center of the robot) is expressed by Equation 3 and Equation 4.

$$\omega=\frac{(V_R-V_L)}{b} \tag{3}$$

$$R = \frac{b}{2}\frac{(V_R+V_L)}{(V_R-V_L)} \quad (4)$$

Using the equation for angular velocity, the instantaneous velocity V of the point located midway between the robot's wheels can be expressed as following Equation 5:

$$V = \omega R \frac{(V_R+V_L)}{2} \quad (5)$$

The tangential velocities of the wheels can also be expressed as:

$$V_R = r\ \omega_R \quad (6)$$

$$V_L = r\ \omega_L \quad (7)$$

In Equation 6 and Equation 7, ω_R and ω_L represent the angular velocities of the right and left wheels, respectively. Consequently, the robot's kinematics in local body coordinates can be expressed as following Equation 8:

$$\begin{bmatrix}\dot{x}\\ \dot{y}\\ \dot{\varphi}\end{bmatrix} = \begin{bmatrix}cos\ \varphi & 0\\ sin\ \varphi & 0\\ 0 & 1\end{bmatrix}\begin{bmatrix}V\\ \omega\end{bmatrix} \quad (8)$$

One might encounter a scenario where the velocity V and the angular velocity ω are provided as inputs, while the angular velocities of the left wheel ω_L and the right wheel ω_R are required as control variables. In this situation, the previously mentioned equations can be easily reformulated. By using the relationships $R=V/\omega$ and $\omega_R=V_R/r$ in following Equation 9:

$$\omega\ \left(R+\frac{b}{2}\right) = V_R \quad (9)$$

One then arrives at the Equation 10 for the angular velocity of the right wheel, ω_R:

$$\omega_R = \frac{V+\omega\ b/2}{r} \quad (10)$$

The similar procedure can also be used to determine the left wheel's angular velocity. Equation 11 shows the angular velocity of the left wheel, ω_L:

$$\omega_R = \frac{V-\omega\ b/2}{r} \quad (11)$$

2.2. Control Methods in the Literature

In this section, controllers in the literature are examined in order to compare the developed controller with existing controllers. The basic equations required for the use of PID (Shah and Agashe 2016), Adaptive PID (Abbas and Mustafa 2024) and Fuzzy Logic (Zangeneh et al., 2022) controllers are given below, respectively. The output values (error values) used in the controllers are equal to the difference between the desired course angle of the differential wheeled robot and the current course angle. The u(t) values obtained from the controllers are the signal values ranging from 0 to 255 sent to the motor controller to move the right and left wheels.

$$u(t) = K_p \times e(t) + K_i \times \int_t^{t+1} e(t)\,dt + K_d \times \frac{de}{dt} \tag{12}$$

Equation 12 shows the PID controller. The values of Kp, Ki and Kd in Equation 12 are constant coefficients of proportional, integral and derivative. These three coefficients must be selected accurately according to the system being controlled. In this study, these three coefficients were selected as 50, 5 and 1, respectively.

$$\begin{aligned} W_R &= max(0, min(255, round(255 + u))) \\ W_L &= max(0, min(255, round(255 - u))) \end{aligned} \tag{13}$$

Equation 13 shows the signal values that should be sent to the right and left wheels, considering the u(t) values coming from the controller in Equation 12. If the differential wheel robot deviates to the left from the desired route, more signals are sent to the left motors, allowing the robot to reach the reference route. Similarly, if the robot deviates to the right from the desired route, more signals are sent to the right motors, allowing the robot to catch the reference route.

$$\begin{aligned} K_p(t+1) &= K_p(t) + P_a \times e(t) \\ K_i(t+1) &= K_i(t) + I_a \times e(t) \\ K_d(t+1) &= K_d(t) + D_a \times e(t) \end{aligned} \tag{14}$$

The difference between the Adaptive PID controller and the classical PID controller is that the constant coefficients Kp, Ki and Kd are defined as a function of time and error value. Equation 14 shows these values used for the Adaptive PID controller.

The following equations show the workflow of the Fuzzy Logic controller. The Fuzzy Logic controller consists of three basic stages: determining the membership functions (triangular), determining the rule base (if-then rules), and calculating the output values (defuzzification).

The membership functions used in fuzzy logic can be defined as shown in Equation 15. The NB value in Equation 15 represents the error value being between -180 and -90, the NS value

represents the error value being between -90 and 0, the NB value represents the error value being between +180 and +90, the PS value represents the error value being between +90 and 0, and the Z value represents the error value being approximately 0.

$$\begin{aligned} \mu_{NB}(e) &= max\left(0, \frac{-e-45}{45}\right) \\ \mu_{NS}(e) &= max\left(0, \frac{-e}{45}\right) \\ \mu_{Z}(e) &= max\left(0, 1 - \frac{|e|}{45}\right) \\ \mu_{PS}(e) &= max\left(0, \frac{e}{45}\right) \\ \mu_{PB}(e) &= max\left(0, \frac{e-45}{45}\right) \end{aligned} \tag{15}$$

The rules of fuzzy logic can be expressed as follows:

1. If error is negative big (NB), right motor is fast, left motor is slow (W_R=PB and W_L=NB).
2. If error is negative small (NS), right motor medium, left motor slow (W_R=PS and W_L=NS).
3. If the error is close to zero (Z), both motors are at equal speed (W_R=Z and W_L=Z).
4. If error is positive small (PS), right motor slow, left motor medium (W_R=NS and W_L=PS).
5. If error is negative small (NS), right motor slow, left motor fast (W_R=NB and W_L=PB).

After the membership functions and rules are determined, the signals that need to be sent to the motors can be calculated with Equation 16 below. Here, μ_i represents the membership degrees and v_i represents the center values of the membership functions.

$$\begin{aligned} W_R &= \frac{\sum_i \mu_i \times v_i}{\sum_i \mu_i} \\ W_L &= \frac{\sum_i \mu_i \times v_i}{\sum_i \mu_i} \end{aligned} \tag{16}$$

2.3. Improvement of an Efficient Controller

Classical PID controllers provide the desired reference value to be captured by taking the proportional, integral and derivative of the error. Since each physical system is different from each other, the 3 coefficient numbers belonging to the proportional, integral and derivative operators must be determined separately for different models. Although numerical simulations are used to determine the optimum values of these three different coefficients, the optimum coefficients obtained from the numerical simulation do not match the optimum coefficients required for differential wheeled robots used in real life due to reasons such as the existence of friction losses, the slipping of the wheels during the first movement or due to different reasons, the battery not always being able to provide the same and constant current and voltage, and the observation of different angular velocities from the

wheels despite the reduction and motors being the same. Experimentally, determining the optimum values of the three coefficients of the PID controller takes a lot of time. For example, when 5 different values of each coefficient are considered, 125 (5^3) experiments are required. This study proposes an effective single-coefficient controller for differential wheeled robots, thus significantly reducing the number of experiments required to achieve optimum control.

Since the differential wheel robot will deviate from the reference route (setpoint) by a maximum of 180 degrees, the reference value is updated with Equation 17 and the output value is adjusted between -180 and +180 degrees:

$$setpoint = \begin{cases} setpoint - 360, & setpoint - input > 180 \\ setpoint + 360, & setpoint - input < -180 \end{cases} \quad (17)$$

Equation 18 shows the determination the error by finding the difference between the setpoint (desired route angle of the differential wheeled robot) and the input (instantaneous heading angle of the differential wheeled robot):

$$error = setpoint - input \quad (18)$$

Equation 19 and Equation 20 express a single coefficient and effective controller developed in this study by taking into account the magnitude of the error value for the differential wheeled robot:

$$W_R = \begin{cases} 75 - error, & error < -L \\ 0, & error > L \\ 255 - 2 \times L - 2 \times error, & -L \leq error \leq L \end{cases} \quad (19)$$

$$W_L = \begin{cases} 0, & error < -L \\ 75 + error, & error > L \\ 255 - 2 \times L + 2 \times error, & -L \leq error \leq L \end{cases} \quad (20)$$

The W_R value and W_L values in Equation 19 and Equation 20 express the signal magnitude given to the right wheel motor and the left wheel motor, respectively. As the W_R and W_L signals increase, the angular speeds of the wheels increase, and as they decrease, the angular speeds decrease. The maximum W_R and W_L values are 255 and the minimum is 0. The L value in Equation 19 and Equation 20 represents the single coefficient that needs to be optimized.

If the error value in Equation 19 and Equation 20 is less than the -L value, the robot has deviated too far from the desired route in a clockwise direction. The robot must turn counterclockwise to catch the reference path. For this reason, the left wheel must stop and the right wheel must move in proportion to the error. Similarly, if the error value is greater than the L value, the robot has deviated too far from the desired route in a counterclockwise direction. The robot must turn clockwise to catch the reference path. For this reason, the right wheel must stop and the left wheel must move in

proportion to the error. If the error value is between -L and +L (the error is relatively smaller than in the above two cases), the robot must be precisely controlled and move forward. For this case, if the error value is 0, both wheels turn with full load and the robot reaches the desired position as soon as possible. If the error value is negative (the robot deviates clockwise), the right wheel is rotated more and the left wheel is rotated less, allowing the robot to catch the reference path. Similarly, if the error value is positive (the robot deviates counterclockwise), the left wheel is rotated more and the right wheel is rotated less, allowing the robot to catch the reference path.

The effect of the L parameter on the differential wheel robot movement can be explained as follows: The first task of the L parameter determines the limit that allows the robot to make a precise movement or a sharp maneuver. If the L parameter is selected small, the robot makes a sharp maneuver even at small error values. Choosing the L value too small can cause oscillatory movement. Oscillatory behavior causes large errors overall. If the L value is selected too large, the reference path is caught too late, and even this situation causes high errors. The second and third duties of the L parameter are to adjust the magnitude of the signals sent to the motor drivers in the precise and sharp maneuver movements of the robot. In this way, the rotation amounts of the right and left wheels are determined as a function of the error and the L parameter.

Duo to the W_R and W_L values obtained in Equation 19 and Equation 20, the rps (revolution per second) of the motors on the right and left is decided by using the “analogWrite” command in the microprocessor. Owing to the accurate W_R and W_L values determined by the proposed effective controller, the differential wheeled robot achieves stable and fast movement.

3. Findings and Discussion

In this study, a single-parameter controller was designed and implemented to move a differential wheel robot. The focus was to find the most suitable value for the "L" parameter, which significantly affects the controller's effectiveness. To evaluate performance, experimental studies were conducted using a robot equipped with an Arduino Nano microprocessor. The differential wheel robot design is illustrated in Figure 2. The front wheels of the robot in Figure 2, marked with red arrows, are driven. The wheels at the back move freely.

Input data were gathered from a digital compass measuring the robot’s heading, while output data were generated by the PWM (Pulse Width Modulation) signals controlling the motors—PWM 6 for the right wheel and PWM 9 for the left. This established a closed-loop control system, ensuring stable control of the robot's movement.

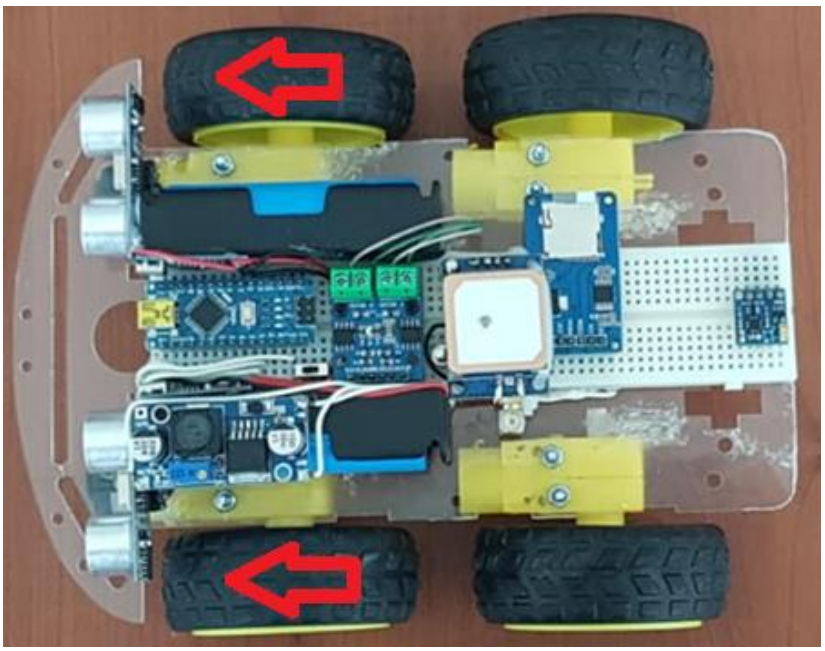

Figure 2. The differential wheel robot design.

Seven experiments were conducted, varying only the "L" parameter, while keeping other conditions constant, including the robot's initial course angle, position, and total distance. The tested "L" values were 38, 40, 43, 44, 45, 46, and 50. The performance was assessed by how quickly and accurately the differential wheel robot could reach a desired heading of 85 degrees. The error between the actual and desired heading, the time to reach the target, and the robot's stability were the key metrics.

The experimental results revealed that L=44 provided the best control, with the robot reaching the target in just 7 seconds with minimal oscillations or overshoot. The data for this trial, including time, heading, and error values, are presented in Table 1. The error was calculated as the difference between the desired heading of 85 degrees and the actual heading at each time step. In contrast, other values of "L" resulted in less stable performance, with the robot exhibiting oscillatory behavior and taking longer to stabilize. Data for these other trials are included in Appendix A.

Table 1. Experimental study for L=44.

L=44											
Time	**Heading**	**Error**	**Time**	**Heading**	**Error**	**Time**	**Heading**	**Error**	**Time**	**Heading**	**Error**
0.00	45	40	2.13	68	17	4.26	78	7	6.39	90	-5
0.30	45	40	2.43	66	19	4.57	81	4	6.70	92	-7
0.61	46	39	2.74	81	4	4.87	85	0	**7.00**	94	-9
0.91	80	5	3.04	83	2	5.17	84	1	**Total Absolute Error**		**312**
1.22	121	-36	3.35	79	6	5.48	94	-9			
1.52	124	-39	3.65	79	6	5.78	90	-5			
1.83	80	5	3.96	80	5	6.09	87	-2			

Figure 3 shows the comparative error values for L=38, L=44, and L=46. The robot's response was stable and quick with L=44 (represented in red), while both L=38 (green) and L=46 (blue) led to oscillations and longer stabilization times. This instability at non-optimal "L" values demonstrates the importance of tuning the parameter carefully.

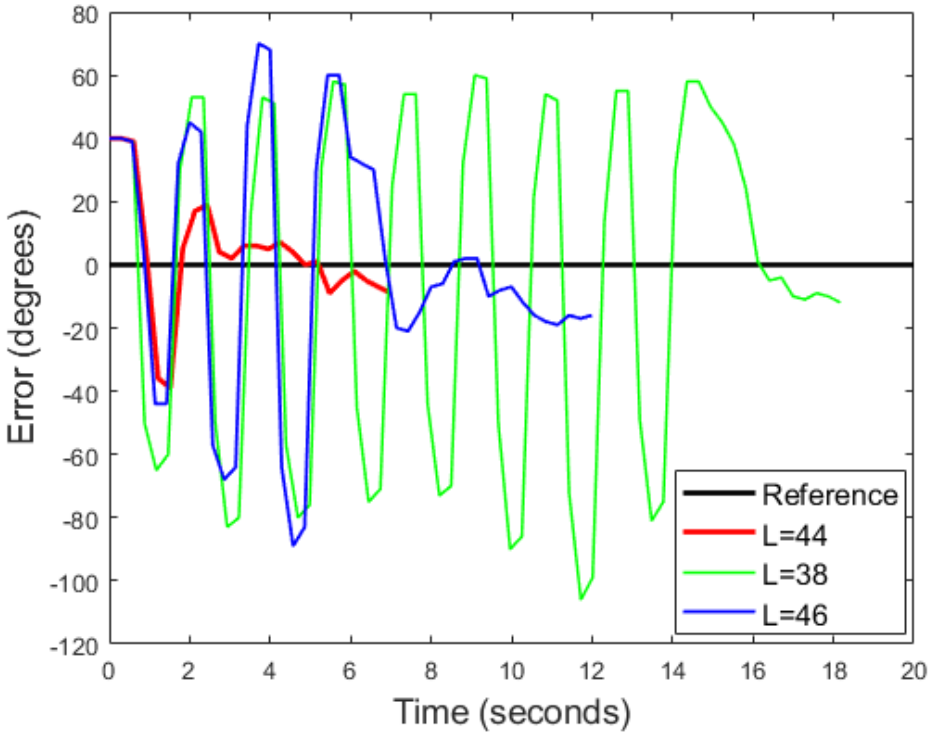

Figure 3. Performance of the designed controller for different L values.

The findings indicate that L=44 is the optimal value for the controller, providing the best balance between responsiveness and stability. Since the error margin of the digital compass used in this study in determining the magnetic field is ±5 degrees, the red colored results (L=44) in Figure 3 indicate that a stable and safe control of the differential wheeled robot is performed. When the "L" parameter is either too high or too low, the robot exhibits unstable and oscillatory movements, which delay the time it takes to reach the desired heading. The data from these trials align with control theory, where poor tuning of control parameters can result in underdamped or overdamped responses. The video links of the robot's movement for L=38, L=44, and L=46, included in Appendix B, further illustrate this point.

The results demonstrate that the "L" parameter is critical to the controller's performance, and the optimal value of L=44 ensures efficient and stable control. Deviating from this value leads to instability and poorer performance. This study underscores the importance of properly tuning control parameters for optimal performance and highlights the need for experimental validation in designing control systems for differential wheel robots.

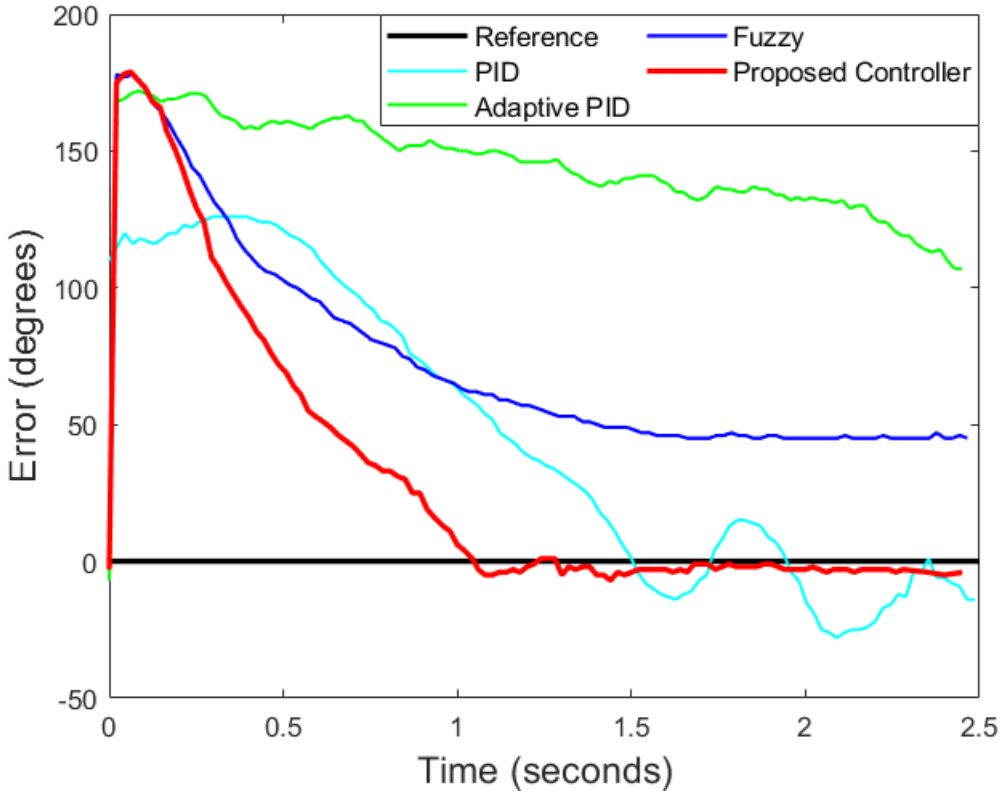

Figure 4. Comparison of the Proposed Controller with PID, Adaptive PID and Fuzzy Logic Controllers (Overshoot=180 degrees).

In this study, the effective and stable behavior of the proposed controller was compared with the classical PID controller, adaptive PID controller and Fuzzy Logic controller in the literature. The experimental results of each controller are given in Figure 4. As seen in Figure 4, a different reference course angle was entered into the differential wheeled robot at t=0 and the performance of each controller in capturing the new course angle was tested. With the entry of the new command, the controller developed in this study can meet the 180-degree deviation (initial course angle=0° and final course angle=180°) that occurs at t=0 in a stable and effective manner and can capture the reference route angle in a shorter time and with less error than other controllers. When the red results in Figure 4 are examined, it is seen that the reference route is captured by the proposed controller with a maximum error of 4 degrees. Since the error margin of the digital compass used in this study in determining the magnetic field is ±5 degrees (the acceptable error margin determined by the manufacturer of the compass is 10 degrees of deviation), the red results in Figure 4 (the results of the proposed controller) show that the differential wheeled robot is controlled stably and safely. The PID controller exhibits an oscillatory behavior on the reference route. The adaptive PID controller is insufficient in capturing the reference angle. Although the Fuzzy Logic controller exhibits stable behavior, it cannot capture the reference path. It is necessary to set the 3 parameters of PID controller (P, I and D), 6 parameters of Adaptive PID controller, namely P, I, D, Pa (proportional adaptation coefficient), Ia (integral adaptation coefficient) and Da (derivative adaptation coefficient) which

provide adaptation of these parameters at each time step, and membership functions, rule numbers and upper and lower limits of membership functions of Fuzzy Logic controller correctly and appropriately. The difficulty of determining each of the multiple parameters of these controllers exactly affects the performance of the controllers negatively. If each parameter could be determined exactly and accurately, of course these controllers would be able to show good performance. However, it is quite difficult to select these multiple parameters accurately only with experimental study and trial-error method. It is clearly seen in Figure 4 that the controller proposed in this study shows effective performance with a few trial and error methods performed in the experimental study with a single parameter in order to overcome these difficulties. In addition to Figure 4, the scenarios of 90-degree deviation at t=0 and deviation from 90 degrees to 270 degrees (180-degree deviation) at t=0 are included in Appendix C and Appendix D, respectively. Full dataset for the comparison of the proposed controller with PID, adaptive PID, and fuzzy logic controllers is included in Appendix E.

The results of three different scenarios were compared with statistical metrics using the mean absolute error (MAE), mean squared error (MSE) and root mean squared error (RMSE) formulas in Equation 21, Equation 22 and Equation 23, respectively. The y_i and r_i in the equations represent the actual (achieved) value (for example, red data in Figure 4) and the reference (target) value (for example, black data in Figure 4), respectively. MAE is suitable for directly understanding the magnitude of errors and when large errors are as important as small ones, while MSE is more appropriate for penalizing large errors more severely, particularly when large errors have significant consequences. RMSE is ideal for assessing the spread of errors or when a more interpretable version of MSE is preferred.

$$MAE = \frac{1}{n}\sum_{i=1}^{n}|y_i - r_i| \tag{21}$$

$$MSE = \frac{1}{n}\sum_{i=1}^{n}\left(y_i - r_i\right)^2 \tag{22}$$

$$RMSE = \sqrt{\frac{1}{n}\sum_{i=1}^{n}\left(y_i - r_i\right)^2} \tag{23}$$

When the results of the three scenarios in Table 2 (Figure 4, Figure A.1 and Figure A.2) are examined, it is clearly seen that the proposed controller provides control of the differential wheeled robot with less error in terms of mean absolute error, mean squared error and root mean squared error compared to other methods.

Table 2. Comparison of the proposed controller using statistical metrics.

		MAE	MSE	RMSE
1st Scenario Figure 4	PID	55.41	5178.71	71.96
	Adaptive PID	144.17	21207.08	145.63
	Fuzzy	73.53	6921.01	83.19
	Proposed	**35.27**	**3953.74**	**62.88**
2nd Scenario Figure A.1	PID	12.74	736.98	27.15
	Adaptive PID	26.81	1188.99	34.48
	Fuzzy	68.88	5447.19	73.81
	Proposed	**8.86**	**572.97**	**23.94**
3rd Scenario Figure A.2	PID	41.54	5559.10	74.56
	Adaptive PID	68.53	5867.59	76.60
	Fuzzy	58.45	4179.13	64.65
	Proposed	**29.78**	**3753.73**	**61.27**

4. Conclusion

This research provides the design and implementation of a novel control system specific to differential wheeled robots, inspired by the widely used PID (Proportional-Integral-Derivative) controller. The main goal was to overcome the significant challenges faced in tuning the three basic parameters—P (Proportional), I (Integral), and D (Derivative)—that are essential for the effective operation of a PID controller. Traditionally, these parameters are carefully tuned using either trial-and-error methods or numerical simulations. Yet, when applied to the real world, this process is revealed to be extremely challenging and even unreliable because of the complexities of reality. Such complexities involve energy losses due to friction, inequalities in current and voltage supply to the direct current motors, and the impossibility of supplying equal angular velocity to the wheels, even if the motors and reduction gearing are identical. In addition, the occurrence of wheel slippage during motion startup and other environmental conditions contribute to the complexity of the situation such that it becomes highly unlikely for the optimum parameters obtained in such a simulated environment to be equal to those needed in actual conditions. In overcoming these challenges, this work proposes a less complex but effective controller comprising a single tunable parameter, thereby obviating the necessity of cumbersome parameter optimization. This controller was developed for differential wheeled robots and was modified to be applied to the specially designed robot model in this study. Emphasizing simplicity and practical implementation, the controller herein suggested facilitates more intuitive and robust tuning by experimental approaches, thereby enhancing its applicability to real-world problems with variability and uncertainty. The experimental phase of this research entailed extensive tests of the new controller implemented on the purposely built differential wheeled robot.

The outcomes indicated that, in spite of the intrinsic challenges faced by real-world applications, the newly developed controller was able to achieve stable, reliable, and effective control of the robot's motion and navigation. This implies that the controller presents a credible option to traditional PID controllers, especially in scenarios where accurate tuning of more than one parameter is not possible or is impossible.

In conclusion, the current research puts forward a novel control method for differential wheeled robots that unifies theoretical developments with practical implementation. Reducing the control architecture to a single adjustable parameter, the controller described herein not only simplifies user convenience but also enables robust and stable performance under real-time dynamic operating environments. This study forms a foundation for the development of more open and robust control systems in the field of robotics, particularly with differential wheeled robots being applied in various applications like autonomous vehicle driving and complicated industrial processes. The controller proposed in this study can be used for different types of robots with large or small differential wheels. Research studies in the future can investigate the applicability of the controller to other robotic platforms and its performance in even more dynamic environments. Additionally, in future studies, more precise controls can be achieved by enhancing the performance of the proposed controller using more sensitive (high-cost) digital compasses.

Statement of Research and Publication Ethics

The author declares that this study complies with Research and Publication Ethics.

References

Abbas, I. A., & Mustafa, M. K. (2024). A review of adaptive tuning of PID-controller: Optimization techniques and applications. International Journal of Nonlinear Analysis and Applications, 15(2), 29-37. https://doi.org/10.22075/ijnaa.2023.21415.4024

Ali, M., Firdaus, A., Arof, H., Nurohmah, H., Suyono, H., Putra, D. & Muslim, M. (2021). The comparison of dual axis photovoltaic tracking system using artificial intelligence techniques. Iaes International Journal of Artificial Intelligence (Ij-Ai), 10(4), 901. https://doi.org/10.11591/ijai.v10.i4.pp901-909

Byeon, Y. J., Jang, M., & Kim, Y. (2025, January). Kinodynamic Modular Approach Local Trajectory Planner for Straightforward Motions of Differential Wheeled Mobile Robots. In 2025 IEEE/SICE International Symposium on System Integration (SII) (pp. 573-580). IEEE.

Carlucho, I., De Paula, M., & Acosta, G. G. (2019). Double Q-PID algorithm for mobile robot control. Expert Systems with Applications, 137, 292-307.

Chung, Y., Park, C., & Harashima, F. (2001). A position control differential drive wheeled mobile robot. IEEE Transactions on Industrial Electronics, 48(4), 853-863.

Díaz-García, G., Giraldo, L. F., & Jimenez-Leudo, S. (2021, October). Dynamics of a differential wheeled robot: control and trajectory error bound. In 2021 IEEE 5th Colombian Conference on Automatic Control (CCAC) (pp. 25-30). IEEE.

Gharghory, S. and Kamal, H. (2012). Optimal tuning of pid controller using adaptive hybrid particle swarm optimization algorithm. International Journal of Computers Communications & Control, 7(1), 101. https://doi.org/10.15837/ijccc.2012.1.1426

Jin, L. (2023). Research on two-stage semi-active isd suspension based on improved fuzzy neural network pid control. Sensors, 23(20), 8388. https://doi.org/10.3390/s23208388

Joseph, S. B., Dada, E. G., Abidemi, A., Oyewola, D. O., & Khammas, B. M. (2022). Metaheuristic algorithms for PID controller parameters tuning: Review, approaches and open problems. Heliyon, 8(5).

Kesavan, E., Gowthaman, N., Tharani, S., Manoharan, S., & Arunkumar, E. (2016). Design and implementation of internal model control and particle swarm optimization based pid for heat exchanger system. International Journal of Heat and Technology, 34(3), 386-390. https://doi.org/10.18280/ijht.340306

Klancar, G., Zdesar, A., Blazic, S., & Skrjanc, I. (2017). Wheeled mobile robotics: from fundamentals towards autonomous systems. Butterworth-Heinemann.

Lee, C. and Chen, R. (2015). Optimal self-tuning pid controller based on low power consumption for a server fan cooling system. Sensors, 15(5), 11685-11700. https://doi.org/10.3390/s150511685

Lee, W., Kim, T., Kim, J., & Seo, T. (2025). Differential-Driven Wheeled Mobile Robot Mechanism with High Step-Climbing Ability. IEEE Robotics and Automation Letters.

Li, B., Ji, Z., Zhao, Z., & Yang, C. (2025). Model Predictive Optimization and Terminal Sliding Mode Motion Control for Mobile Robot With Obstacle Avoidance. IEEE Transactions on Industrial Electronics.

Mohanty, P. K., & Parhi, D. R. (2013). Controlling the motion of an autonomous mobile robot using various techniques: a review. Journal of Advance Mechanical Engineering, 1(1), 24-39.

Mújica-Vargas, D., Vela-Rincón, V., Luna-Álvarez, A., Rendón-Castro, A., Matuz-Cruz, M., & Rubio, J. (2022). Navigation of a differential wheeled robot based on a type-2 fuzzy inference tree. Machines, 10(8), 660.

Ortenzi, V., Marturi, N., Mistry, M., & Kuo, J. (2018). Vision-based framework to estimate robot configuration and kinematic constraints. Ieee/Asme Transactions on Mechatronics, 23(5), 2402-2412. https://doi.org/10.1109/tmech.2018.2865758

Qu, S., He, T., & Zhu, G. (2023). Model-assisted online optimization of gain-scheduled pid control using nsga-ii iterative genetic algorithm. Applied Sciences, 13(11), 6444. https://doi.org/10.3390/app13116444

Raj, M. and Seamans, R. (2019). Primer on artificial intelligence and robotics. Journal of Organization Design, 8(1). https://doi.org/10.1186/s41469-019-0050-0

Sahu, P. and Prusty, R. (2018). Performance enhancement in agc of multi-area power system with woa optimized fo-2dof controller and facts controllers. International Journal of Engineering & Technology, 7(3.3), 562. https://doi.org/10.14419/ijet.v7i2.33.14835

Salman, G., Jafar, A., & Ismael, A. (2019). Application of artificial intelligence techniques for lfc and avr systems using pid controller. International Journal of Power Electronics and Drive Systems (Ijpeds), 10(3), 1694. https://doi.org/10.11591/ijpeds.v10.i3.pp1694-1704

Shah, P., & Agashe, S. (2016). Review of fractional PID controller. Mechatronics, 38, 29-41.

Somefun, O. A., Akingbade, K., & Dahunsi, F. (2021). The dilemma of PID tuning. Annual Reviews in Control, 52, 65-74.

Tahtawi, A., Putri, F., & Martin, M. (2023). Position control of ax-12 servo motor using proportional-integral-derivative controller with particle swarm optimization for robotic manipulator application. Iaes International Journal of Robotics and Automation (Ijra), 12(2), 184. https://doi.org/10.11591/ijra.v12i2.pp184-191

Ye, L., Hou, Y., & Li, D. (2017). Genetic algorithm's application for optimization of pid parameters in dynamic positioning vessel. Matec Web of Conferences, 139, 00153. https://doi.org/10.1051/matecconf/201713900153

Zangeneh, M., Aghajari, E., & Forouzanfar, M. (2022). A review on optimization of fuzzy controller parameters in robotic applications. IETE Journal of Research, 68(6), 4150-4159.

Zhang, J. (2015). Improved decoupled nonminimal state space model based pid for multivariable processes. Industrial & Engineering Chemistry Research, 54(5), 1640-1645. https://doi.org/10.1021/ie504314c

Zhang, J., Liu, J., Liu, B., & Li, M. (2022). Fractional order pid control based on ball screw energy regenerative active suspension. Actuators, 11(7), 189. https://doi.org/10.3390/act11070189

Zhu, Z., Kaizu, Y., Furuhashi, K., & Imou, K. (2021). Visual-inertial RGB-D SLAM with encoders for a differential wheeled robot. IEEE Sensors Journal, 22(6), 5360-5371. https://doi.org/10.1109/JSEN.2021.3101370

Appendix A

Table A1. Experimental study for L=38.

L=38											
Time	**Heading**	**Error**	**Time**	**Heading**	**Error**	**Time**	**Heading**	**Error**	**Time**	**Heading**	**Error**
0.00	45	40	4.98	161	-76	9.96	175	-90	14.95	35	50
0.29	45	40	5.28	54	31	10.26	171	-86	15.24	40	45
0.59	46	39	5.57	27	58	10.55	64	21	15.53	47	38
0.88	135	-50	5.86	28	57	10.84	31	54	15.83	61	24
1.17	150	-65	6.15	130	-45	11.14	33	52	16.12	84	1
1.47	145	-60	6.45	160	-75	11.43	157	-72	16.41	90	-5
1.76	55	30	6.74	156	-71	11.72	191	-106	16.70	89	-4
2.05	32	53	7.03	60	25	12.02	184	-99	17.00	95	-10
2.34	32	53	7.33	31	54	12.31	71	14	17.29	96	-11
2.64	135	-50	7.62	31	54	12.60	30	55	17.58	94	-9
2.93	168	-83	7.91	129	-44	12.89	30	55	17.88	95	-10
3.22	165	-80	8.21	158	-73	13.19	134	-49	**18.17**	97	-12
3.52	69	16	8.50	155	-70	13.48	166	-81	**Total Absolute Error**		**3108**
3.81	32	53	8.79	53	32	13.77	160	-75			
4.10	34	51	9.09	25	60	14.07	55	30			
4.40	142	-57	9.38	26	59	14.36	27	58			
4.69	165	-80	9.67	135	-50	14.65	27	58			

Table A2. Experimental study for L=40.

L=40											
Time	**Heading**	**Error**	**Time**	**Heading**	**Error**	**Time**	**Heading**	**Error**	**Time**	**Heading**	**Error**
0.00	44	41	2.34	89	-4	4.68	129	-44	7.01	82	3
0.29	44	41	2.63	225	-140	4.97	125	-40	7.31	85	0
0.58	46	39	2.92	43	42	5.26	111	-26	7.60	88	-3
0.88	63	22	3.21	32	53	5.55	94	-9	**7.89**	85	0
1.17	95	-10	3.51	122	-37	5.84	94	-9	**Total Absolute Error**		**775**
1.46	103	-18	3.80	145	-60	6.14	94	-9			
1.75	97	-12	4.09	143	-58	6.43	87	-2			
2.05	88	-3	4.38	134	-49	6.72	84	1			

Table A3. Experimental study for L=43.

L=43											
Time	**Heading**	**Error**	**Time**	**Heading**	**Error**	**Time**	**Heading**	**Error**	**Time**	**Heading**	**Error**
0.00	45	40	3.00	100	-15	6.00	89	-4	9.00	75	10
0.30	45	40	3.30	92	-7	6.30	82	3	9.30	74	11
0.60	45	40	3.60	75	10	6.60	71	14	9.60	76	9
0.90	67	18	3.90	71	14	6.90	71	14	9.90	79	6
1.20	118	-33	4.20	74	11	7.20	72	13	10.20	80	5
1.50	125	-40	4.50	96	-11	7.50	71	14	**10.50**	77	8

1.80	73	12	4.80	97	-12	7.80	71	14	**Total Absolute Error**	**554**
2.10	58	27	5.10	95	-10	8.10	70	15		
2.40	61	24	5.40	91	-6	8.40	71	14		
2.70	97	-12	5.70	90	-5	8.70	72	13		

Table A4. Experimental study for L=45.

L=45											
Time	**Heading**	**Error**	**Time**	**Heading**	**Error**	**Time**	**Heading**	**Error**	**Time**	**Heading**	**Error**
0.00	44	41	2.13	54	31	4.26	85	0	6.39	91	-6
0.30	45	40	2.43	59	26	4.57	83	2	6.70	92	-7
0.61	45	40	2.74	100	-15	4.87	85	0	**7.00**	91	-6
0.91	80	5	3.04	104	-19	5.17	90	-5	**Total Absolute Error**		**365**
1.22	125	-40	3.35	96	-11	5.48	89	-4			
1.52	127	-42	3.65	86	-1	5.78	88	-3			
1.83	68	17	3.96	87	-2	6.09	87	-2			

Table A5. Experimental study for L=46.

L=46											
Time	**Heading**	**Error**	**Time**	**Heading**	**Error**	**Time**	**Heading**	**Error**	**Time**	**Heading**	**Error**
0.00	45	40	3.43	41	44	6.86	83	2	10.29	97	-12
0.29	45	40	3.71	15	70	7.14	105	-20	10.57	101	-16
0.57	46	39	4.00	17	68	7.43	106	-21	10.86	103	-18
0.86	81	4	4.29	149	-64	7.71	100	-15	11.14	104	-19
1.14	129	-44	4.57	174	-89	8.00	92	-7	11.43	101	-16
1.43	129	-44	4.86	168	-83	8.29	91	-6	11.71	102	-17
1.71	53	32	5.14	55	30	8.57	84	1	**12.00**	101	-16
2.00	40	45	5.43	25	60	8.86	83	2	**Total Absolute Error**		**1398**
2.29	43	42	5.71	25	60	9.14	83	2			
2.57	142	-57	6.00	51	34	9.43	95	-10			
2.86	153	-68	6.29	53	32	9.71	93	-8			
3.14	149	-64	6.57	55	30	10.00	92	-7			

Table A6. Experimental study for L=50.

L=50											
Time	**Heading**	**Error**	**Time**	**Heading**	**Error**	**Time**	**Heading**	**Error**	**Time**	**Heading**	**Error**
0.00	45	40	6.49	148	-63	12.99	188	-103	19.48	139	-54
0.28	45	40	6.78	66	19	13.27	187	-102	19.76	178	-93
0.56	45	40	7.06	37	48	13.55	74	11	20.05	172	-87
0.85	85	0	7.34	34	51	13.84	28	57	20.33	57	28
1.13	133	-48	7.62	108	-23	14.12	30	55	20.61	23	62
1.41	132	-47	7.91	142	-57	14.40	149	-64	20.89	25	60
1.69	47	38	8.19	141	-56	14.68	177	-92	21.18	140	-55
1.98	31	54	8.47	46	39	14.96	171	-86	21.46	190	-105

2.26	35	50	8.75	24	61	15.25	54	31	21.74	185	-100
2.54	165	-80	9.04	27	58	15.53	24	61	22.02	54	31
2.82	218	-133	9.32	150	-65	15.81	30	55	22.31	18	67
3.11	213	-128	9.60	186	-101	16.09	147	-62	22.59	20	65
3.39	93	-8	9.88	175	-90	16.38	185	-100	22.87	141	-56
3.67	35	50	10.16	56	29	16.66	182	-97	23.15	199	-114
3.95	33	52	10.45	22	63	16.94	55	30	23.44	191	-106
4.24	139	-54	10.73	22	63	17.22	24	61	23.72	54	31
4.52	162	-77	11.01	100	-15	17.51	29	56	**24.00**	3	82
4.80	158	-73	11.29	142	-57	17.79	141	-56	**Total Absolute Error**		**5157**
5.08	51	34	11.58	141	-56	18.07	179	-94			
5.36	17	68	11.86	54	31	18.35	173	-88			
5.65	17	68	12.14	31	54	18.64	57	28			
5.93	97	-12	12.42	39	46	18.92	29	56			
6.21	146	-61	12.71	149	-64	19.20	33	52			

Appendix B

Google Drive Links of videos for experimental studies (L=38, L=44 and L=46):

https://drive.google.com/drive/folders/1pXxIzxSv4E4pwutwl6YH3U22_t25BFmo?usp=sharing

Appendix C

The 90-degree deviation (initial course angle=180° and final course angle=90°) that occurs at t=0:

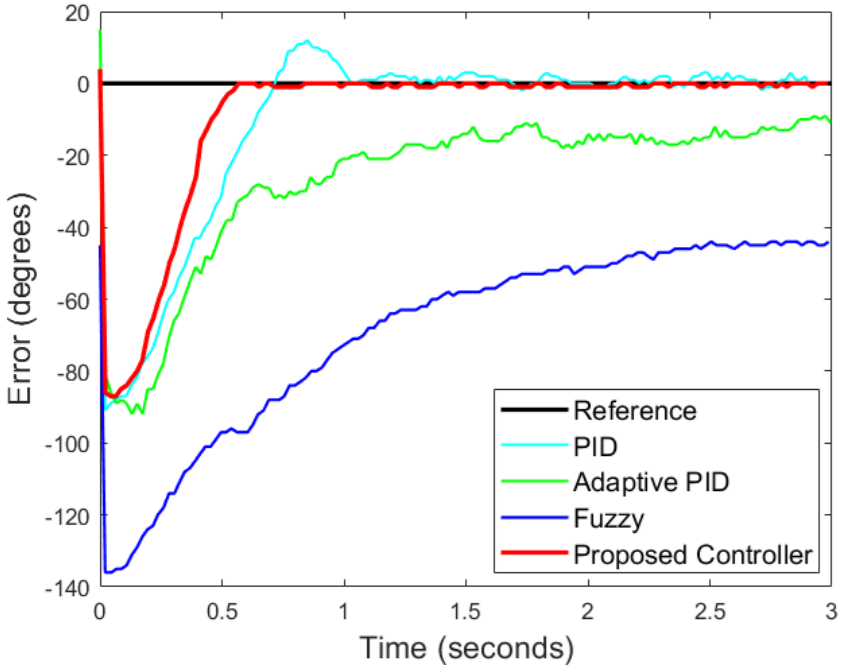

Figure A.1. Comparison of the Proposed Controller with PID, Adaptive PID and Fuzzy Logic Controllers (Overshoot=90 degrees).

Appendix D

The 180-degree deviation (initial course angle=90° and final course angle=270°) that occurs at t=0:

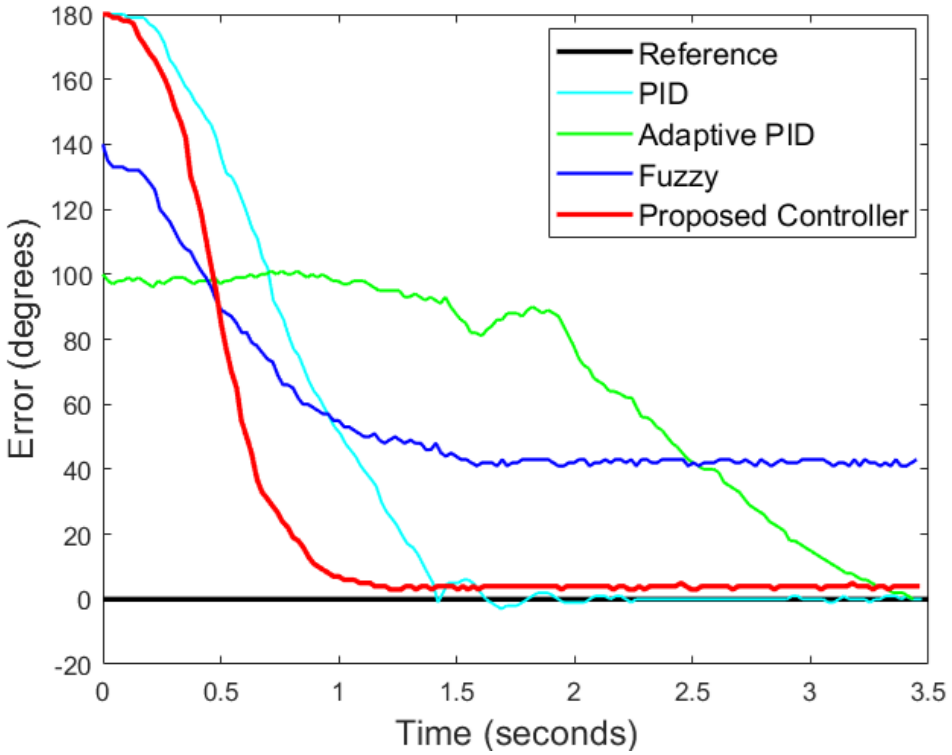

Figure A.2. Comparison of the Proposed Controller with PID, Adaptive PID and Fuzzy Logic Controllers (Overshoot=180 degrees).

Appendix E

Full dataset for the comparison of the proposed controller with PID, adaptive PID, and fuzzy logic controllers:

https://drive.google.com/drive/folders/1hKw95cPygUFsar3mX7LvEBrtELQxxL96?usp=sharing